



ORIGINAL RESEARCH ARTICLE

MAPPING AND STIMULATING FLASH FLOOD IN THE CATCHMENT OF
JUKSKIE RIVER

R. Sithole, E. K. Onyari, and G. U. Fayomi *

Department of Civil and Environmental Engineering and Building Sciences, University of South Africa, Florida
Science Campus, Cnr Christian de Wet Road and Pioneer Avenue, Johannesburg, South Africa

*Corresponding author's email: fayomiuche@gmail.com

ARTICLE INFORMATION

Received: 19th June 2025
Revised: 12th July 2025
Accepted: 14th July 2025

Keywords:

Flooding
Juskskei river
GIS
Mapping
Remote sensing

ABSTRACT

Flash floods are among the most severe hydrological hazards, posing significant threats to urban areas worldwide. This study focuses on flash flood mapping of Jukskei River, a catchment in Johannesburg, South Africa, prone to frequent flash flooding. The study employed combination of remote sensing and GIS techniques. The approach follows an analytical framework using satellite imagery and Digital Elevation Models (DEMs) Major extreme rainfall events were analyzed such as rainfall covering 241.6 mm (over 6 hours) and 122 mm (over 4 hours)—corresponding to return periods of 100 and 50 years, respectively. The results of the HEC-RAS simulation were integrated into QGIS to visualize the spatial extent of flooding for the rainfall intensities. The DEM data was processed to identify areas prone to overland flow accumulation, and flood extents were mapped based on the water surface elevations calculated for the 40.27 mm/h and 30.5 mm/h intensities. The mapping results highlighted critical zones where water levels exceeded the riverbanks, potentially endangering residential areas and infrastructures. The findings emphasized the importance of integrated flood risk management strategies to mitigate future hazards and enhance urban resilience.

© 2025 Faculty of Engineering, University of Maiduguri, Nigeria. All rights reserved.

1.0 Introduction

Flash floods have become one of the most dangerous and common natural disasters in the world, especially in metropolitan areas where the issue is made worse by fast growth and shifting climate conditions (Kaplan and Avdan, 2018). Its speedy start off, distressing effects, massive infrastructure destruction, economic disruption and loss of human lives are characteristics of its nature (Agonafor et al., 2023). A combination of inadequate drainage infrastructure, growing urbanization, and erratic weather patterns brought on by climate change is making flash floods increasingly common (Mutuvhi et al., 2020). Usually, flash floods occur when precipitation surpasses the ability of the land or urban drainage systems to absorb water, resulting in abrupt and intense water surges (Baloyi et al., 2018; Lin et al., 2021). Unlike regular flooding, flash floods happen quickly, often without warning, and have devastating environmental repercussions, infrastructure, human life, and ecosystem as a whole. Flash floods are one of the main natural disasters that contribute to a higher death rate worldwide, according to the World Health Organization (WHO), (Bucherei et al., 2022).

Flash flood delinquent has worsened recently due to fast urbanization surrounding the Jukskei River catchment, which has deteriorated given the exposure of hard sub-surface rocks that have characteristically low infiltration rates and pave way to large surface runoff during periods of intense rainfall (Fadupin et al., 2022). Furthermore, the frequency of its occurrences is attributed to the available malfunctioning drainage systems that are unable to handle the unexpected surge of storm water volume (Teffo et al., 2023). Flash flood situations pose negative effect on public and private buildings, roadways infrastructures, affecting transportation networks leading to financial burdens for road infrastructures while it creates further exacerbates socioeconomic problems, ecological imbalance, public health hazards, including water related illnesses and complications (Franssen, 2025; Mawasha and Britz, 2021). Globally, urban planners, emergency services, and legislators are working continuously to identify the mitigation techniques towards reduction of flash floods (Alarifi et al., 2022; Guo et al., 2021).

Recently, the use of GIS and satellite images in flood management approaches has been revolutionized by available satellite data and analysis methods (Kaplan and Avdan, 2018). Large areas may be observed from satellite imagery on board, which makes it possible to track land cover, water bodies, and the progressions of flooding events in almost real time. Radar and multispectral satellite sensors, including those on Sentinel-1, Sentinel-2, and Landsat-8, have made it possible to monitor flash floods and acquire data on possible management (Schlaffer *et al.*, 2015; Moeketsi *et al.*, 2022). Dube *et al.*, (2020) utilized GIS-based hydrological modeling to predict flood behavior in metropolitan areas. Their work accurately identified flood-prone locations by simulating flood propagation using rainfall data and Digital Elevation Models (DEMs). Mutuvhi *et al.*, (2020) used a multi-criteria decision-making model based on GIS to evaluate the Yarlung Zangbo river basin's susceptibility to flash floods. This approach identified the area's that are most susceptible to flash floods based on environmental data related to soil topography, anthropogenic, and the climate changing situations.

Similarly, GIS-based models that take into consideration changes in land use, rainfall patterns, and hydrological features have been used to evaluate flood hazards in South African cities (Abdelkareem *et al.*, 2022); (Mutuvhi *et al.*, 2020). These methods have been successful in locating high-risk locations, giving risk managers and urban planners useful resources (Mutuvhi *et al.*, 2020). By superimposing several datasets, such as satellite imageries, Digital Elevation Models (DEMs), and meteorological data, GIS enables the identification of locations that are vulnerable to flooding. This application facilitates the creation of thorough flood risk assessments and early warning systems (Lin *et al.*, 2021). Nevertheless, there are still gaps in the integration of environmental data in the Jukskei river watershed, despite the significant advancements in the use of satellite imaging and GIS for flood risk assessment. Similarly, in refining rainfall thresholds for different catchments and integrating participatory GIS approaches to engage local communities could enhance the usefulness of flood risk maps in South Africa. Therefore, this study focused on utilizing satellite imagery and GIS to map high-risk areas along the Jukskei River. The study's main objectives were to determine which regions are most vulnerable to flash floods, examine how urbanization affects flood behavior, and create maps of flood hazards that disaster management organizations and urban planners can use.

2. Study Area

Rapid urbanization has drastically changed the natural landscape in the heavily populated urban area where the Jukskei water basin is situated (Mutuvhi *et al.*, 2020). There are a lot of impermeable surfaces including roads, buildings, and parking lots across the catchment, which consists of a mix of urban, semi-urban, and peri-urban areas accelerating storm water runoff and increasing the risk of flash flooding. The river basin spans over 700 square kilometers, from Johannesburg's northern suburbs to the point where it meets the Crocodile River (Mawashi and Britz, 2021; Kaplan and Avdan, 2018). Because of the topographical gradient and periods of high rainfall, which enable water to amass quickly, the area is susceptible to flash floods (Arabameri *et al.*, 2020). The summer rainfall pattern of the area is what defines its climate, with most of the severe downpours taking place between November and March. These climatic circumstances, attached with the area's topography terrain and inadequate urban infrastructure, formed a perfect storm for flash flooding (Mutuvhi *et al.*, 2020). Figure 1 revealed the locality map of Jukskei river. The location of the river catchment and the existing informal settlements and subpar housing made the villages more susceptible to flash floods. (Arabameri *et al.*, 2020).

2.1 Natural Features of Jukskei Catchment

Jukskei catchment featured a mean annual rainfall (MAP) of 713 mm and unpredictable seasonal rainfall patterns with a mild climate condition (Mawasha and Britz, 2021). The catchment has seasonal variations in temperature, with summertime minimums and maximums between 14°C and 25°C, and cold wintertime minimums and maximums between 0°C and maximum temperatures peak to 17 °C (Moeketsi *et al.*, 2022). Similarly, Jukskei area featured two vegetation biomes, which is the grassland and savanna biomes (Mawasha and Britz, 2021). The vegetation categories having the most alteration the catchment include Rand Highveld Grassland, Gauteng Shale Mountain Bushveld and Egoli Granite Grassland. the catchment's soil types can be roughly categorized as clayey loams ranging from mild to deep. When enough water is available, the majority of clayey loam soils, in particular, are ideal for commercial agriculture (Kaplan and Avdan, 2018). Flood frequency, depth and velocity in Jukskei River catchment have significantly increased over time, according to analysis, and the depth-velocity product has also increased significantly caused by factors such as changes in land use and urbanization (Mawasha and Britz, 2021).

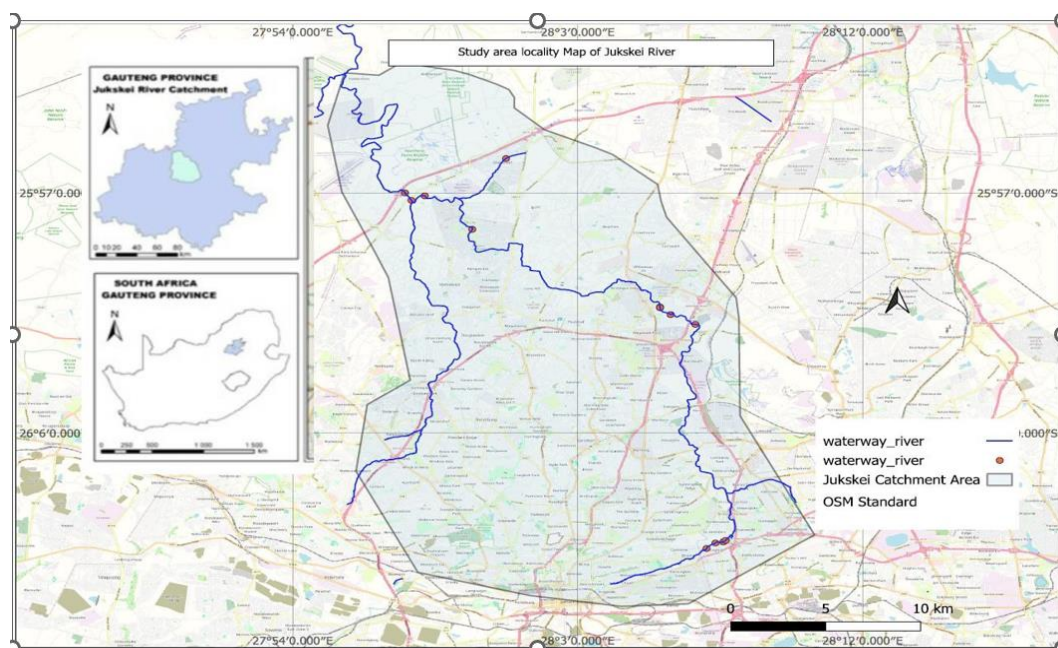


Figure 1: Locality map of Jukskie River

2.2 Hydrological Characteristics

The Jukskei River is a perennial surface water body whose discharge fluctuates throughout annually. Under typical circumstances, the river acts as a vital conduit for the drainage of Johannesburg's stormwater and wastewater (Teffo *et al.*, 2023). However, the river's capacity is frequently surpassed during periods of high intensity rainfall events, resulting in flash floods that destroy infrastructures and disturb urban life (Abiye, 2023).

2.3 Flood Vulnerability

Flooding is a major concern at the downstream the Jukskei River, especially in the catchment's center and northern regions (Nenweli *et al.*, 2024). The absence of resilient infrastructures such as adequate drainage channels makes the location vulnerable to floodwaters, the informal communities along riverbanks are particularly vulnerable Mawasha and Briz 2023; Aarbameri *et al.*, 2020). Furthermore, the floodplain is intersected by vital infrastructure, such as pipelines, bridges, and major roadways, rendering these places vulnerable to substantial disruptions during flood occurrences (Nenweli *et al.*, 2024). Similarly, due to strong thunderstorms, the Jukskei River floods regularly, particularly from October to March during the summer (Mawasha and Britz, 2021). Parts of the river downstream are furrowed with parks and greenery zones like Jukskei Park. It also featured partial downstream agricultural practice due to urbanization and resultant urban sprawl. However, high density residential pattern and informal settlement are common around Jukskei catchment (Sheree, 2024). These communities are highly susceptible to flash flood occurrences due to proximity to the river and poor drainage system. Drainage type in the settlement includes both piped drainage system and the natural drainage such retention ponds, wetlands and storm water drain network (Malatji, 2019) however, all the available drainage facilities are poorly maintenance, encroachment, blocked or filled therefore, reducing flood management efficiency (Moektsi *et al.*, 2023; Malatji, 2019).

3. Methodology

Remote sensing, GIS tools combined with historical data were employed in this research. The method uses digital elevation models (DEMs) and satellite imagery as part of an analytical framework (Hussein *et al.*, 2019; Alarifi *et al.*, 2022). Flood behavior, including water flow, was simulated using the hydrological modeling software HEC-RAS, which also produced flood hazard maps for return periods of 20, 50, and 100 years. Data on topography was obtained from Shuttle Radar Topography Mission (SRTM) 30m Digital Elevation Model (DEM) for the Jukskei River catchment analyzed using QGIS software. 5years rainfall and streamflow data were retrieved from SAWS and DWS databases, with more attention to extreme rainfall events for threshold analysis: Rainfall data were analyzed to categorize rain events exceeding the 60 mm/day threshold therefore, threshold method was adopted for the calculation of surplus rainfall shown in equation 4. This is critical for prompting flash floods. Similarly, Normalized Difference Moisture Index (NDMI) was also derived from Sentinel 2 band for soil moisture analysis using spectral band of short-wave infrared (SWIR) and near infrared

(NIR) wavelengths. The NDMI formular used is shown in equation 1. Gumbel distribution formula was utilized in estimating the rainfall return periods. The formular for Gumbel distribution is declared in equation 2.

$$NDMI = \frac{(P_{NIR} - P_{SWIR})}{(P_{NIR} + P_{SWIR})} = \frac{(B_8 - B_{11})}{(B_8 + B_{11})} \quad 1$$

where B8 is the near-Infrared (NIR) band (central wavelength ~842 nm) and B11 is short-Wave Infrared (SWIR) band (central wavelength ~1610 nm).

$$\vec{I} = \mu + \sigma \times (-\ln(I - \frac{1}{T})) \quad 2$$

Where μ is the mean rainfall (66.48 mm), σ is the standard deviation (46.22 mm), and T is the return period (20, 50, or 100 years).

Rational Method formula was also utilized to capture water catchment area, and a runoff coefficient for urban catchments. The formular is shown in equation 3, 4 and 5

$$Q = C \times I \times A \quad 3$$

where C=0.8 (runoff coefficient for urban catchments), I is the intensity in mm/h. (assume that the rainfall is concentrated over 4 hours in a day) and A is the catchment area (2,000 km², converted to hectares).

$$Rainfall\ surplus = Actual\ Rainfall - Threshold\ Rainfall \quad 4$$

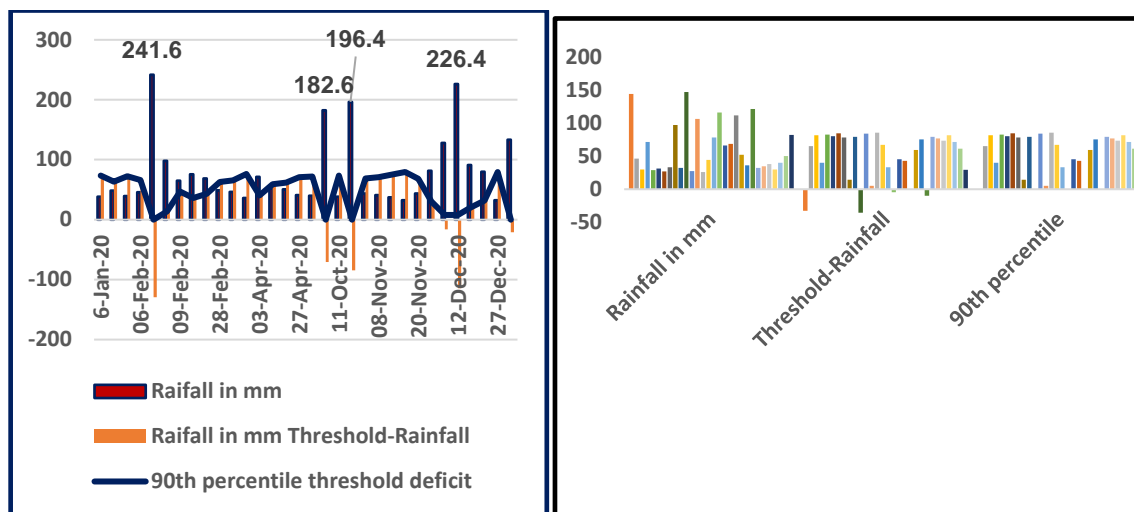
However

$$Rainfall\ Dificit = Threshold\ Rainfall - Actual\ Rainfall \quad 5$$

Physical flood verification was conducted using real-time media evidence retrieved online covering both ground survey and observational data.

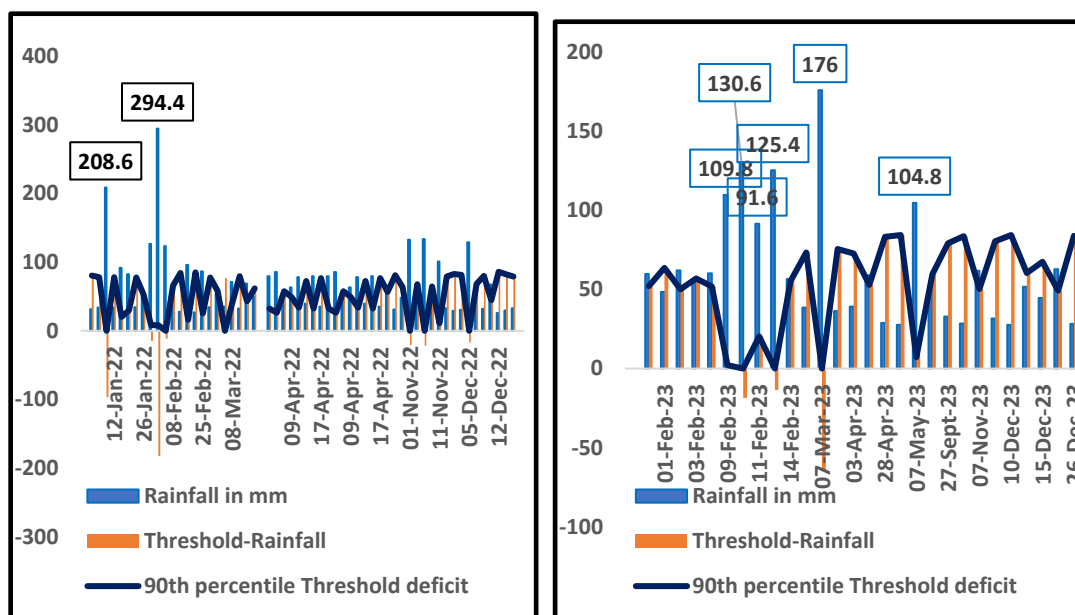
4. Results and Discussion

The outcome of the rainfall trend in Jukskei catchment for each year showing notable surplus events in different years driven mostly by intense rainfall situation. These conditions directly heighten the risk of flash flooding given the paucity of other environmental situations such as runoff intensity, soil permeability, evapotranspiration, topography and slope terrain (Razavi-Termeh et al., 2023). Statistical analysis displayed decreasing surplus trend event from 2020 -2024 indicating higher frequency of lower normal rainfall with significant irregular distributions. Higher peak rainfall occurred mostly in 2020, 2022 and 2023. Surplus rainfall was equally witnessed in all the year with higher record in 2020, 2021 and 2022 Figure Similarly, maximum rainfall was recorded in 2020 amounting to 78.03mm, followed by 2022 with 65.1mm. The likelihood of a flood increases as the amount of rainfall at a given location rises (Abiye, 2023). This is because higher rainfall intensity generates greater volumes of water over a short period. Rainfall data breakdown for the study period calculated revealed a sum of 10104.5 mm, average (mean) 66.48 mm (median) 48.9 mm (standard deviation) 46.22 mm. The daily rainfall data was filtered for heavy rain events, thresholds are often set based on the rainfall's potential to cause flooding (Zebe and Sivapalan, 2009). 90th percentile-based thresholds commonly used to differentiate between normal and substantial rainfall events was utilized to detect the trend. Figure 2 (a-e) revealed rainfall per days analyzed from the data gathered using a 90% threshold. Critical periods when rainfall surplus rises such as situations where precipitation substantially surpasses the threshold, indicating significant implications for flash flood risk evaluation (Hosseini, 2024). The highest rainfall data points (50) and maximum rainfall (294.4 mm) occurred in 2022, Table 1, resulting in seven surplus days. However, the overall surplus (14 mm) was still low, most likely as a result of higher Potential Evapotranspiration (PET) or faster soil absorption. 2020 and 2021 also recorded significant rainfall data points (32) (29) respectively with six surplus days which are very closer to 2022. Figure 2 (a-e) revealed the outcome of trend in Jukskei river catchment. Figure 3a shows deficit vs surplus rainfall.



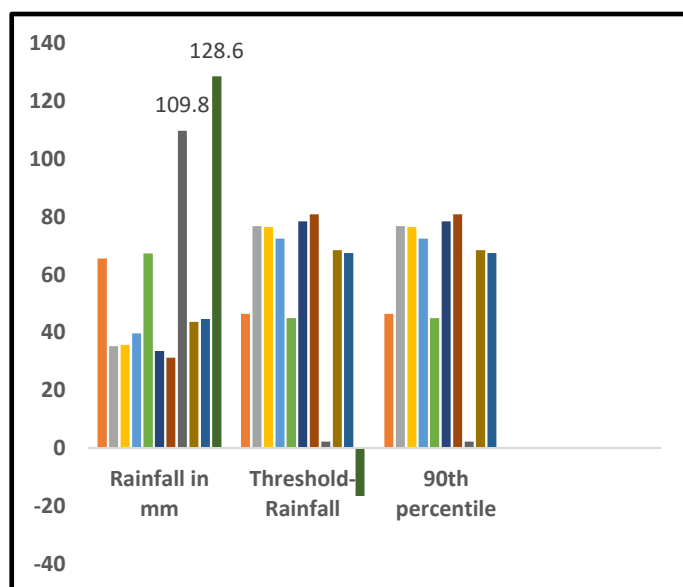
(a) 2020

(b) 2021



(c) 2022

(d) 2023



(e) 2024

Figure 2: (a-e) Rainfall (mm) per day graph (2020-2024)

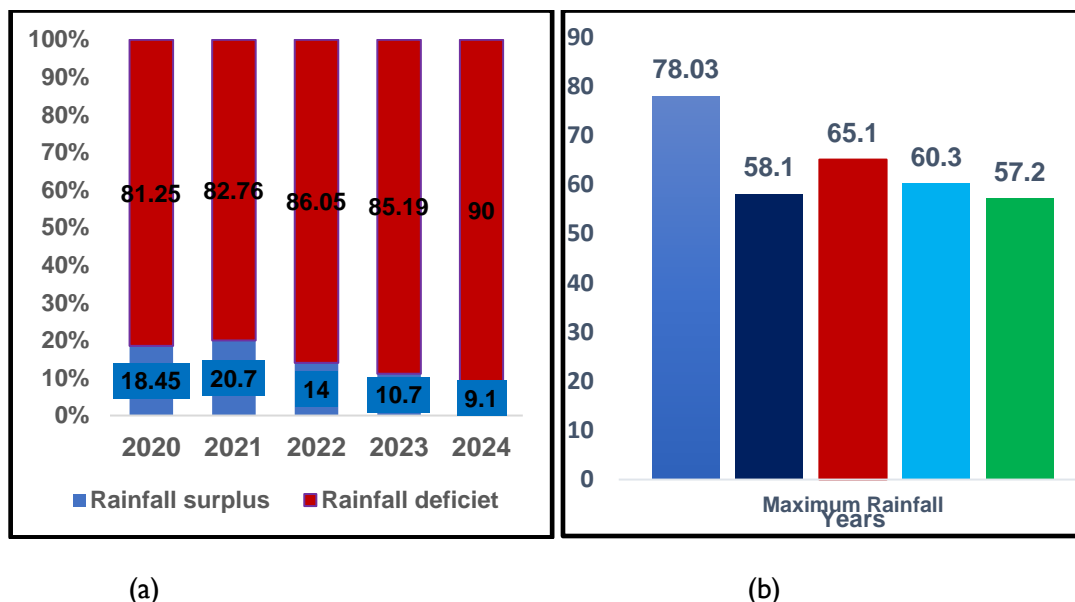


Figure 3: Showing (a) deficit vs surplus rainfall (b) rainfall trend

Table I: Rainfall trend 2020-2024

Year	Data point	Average rainfall (mm)	Max rainfall (mm)	Surplus days	% Surplus	% Deficit
2020	32	78.03	241.6	6	18.47	7.25
2021	29	58.1	147.6	6	20.7	80.06
2022	50	65.1	294.4	7	14	86.05
2023	28	60.3	176	3	10.7	85.19
2024	14	57.2	128.6	1	9.1	90

The data from Sentinel-2 with the use of Normalized Difference Moisture Index showed a clear correlation between high moisture levels and flood-prone areas along the Jukskei River, especially in the floodplain regions, Figure 4

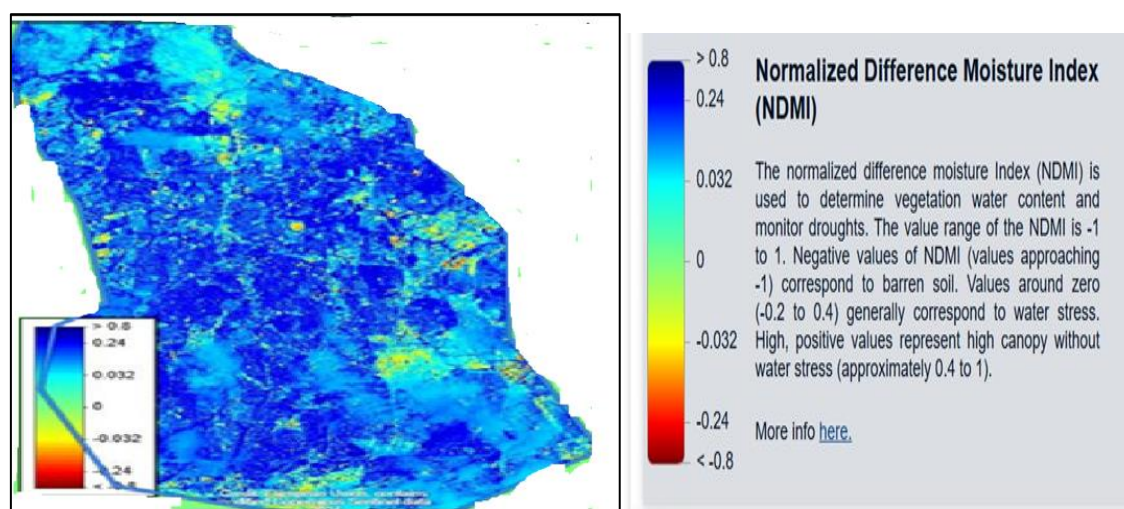


Figure 4: Soil moisture map

Flood-prone zones along the river displayed high moisture indices after the flood events of 4-Feb- 22, 7-Feb-20, 12-Dec-20, 7-Jan-22 consistent with the periods of flooding identified in the rainfall dataset characterized of soils with lower permeability. This result aligned with previous studies on soil influence on flooding (Sellame *et al.*, 2024; Lin *et al.*, 2021). The elevation map and slope analysis Figure 5 (a and b), of the catchment exhibits a marked contrast between highland areas (with steep slopes) and lowland areas (along the river valley situated in the Highveld area of South Africa. The topography of Johannesburg's northern suburbs is distinguished by an undulating profile made up of several "koppies." The elevation of these koppies ranges from 1 450 to 1 600 m.a.s.l. in the northeast and from 1 33 275 to 1 450 m.a.s.l. in the northwest (Moeketsi *et al.*, 2022). This variation in topography significantly influences how water flows across the landscape, affecting the potential for flooding (Mukherjee and Singh, 2020). Figure 5c displays the LULC map for Jukskei River catchments created in this study using QGIS and the available remote sensing data (ESRI Land Cover 2023) The result revealed greater increase in built-up area ranging more than 50% and decrease in vegetation cover which could result to low infiltration of rainwater. Urban areas with impermeable surfaces, such as roads, buildings, and parking lots, are among the main land cover categories found in the study area. These surfaces stop water from penetrating the ground and increase surface runoff during rainfall events, which is a major cause of flash flooding (Anaba *et al.*, 2017; Pedzisai, 2016).

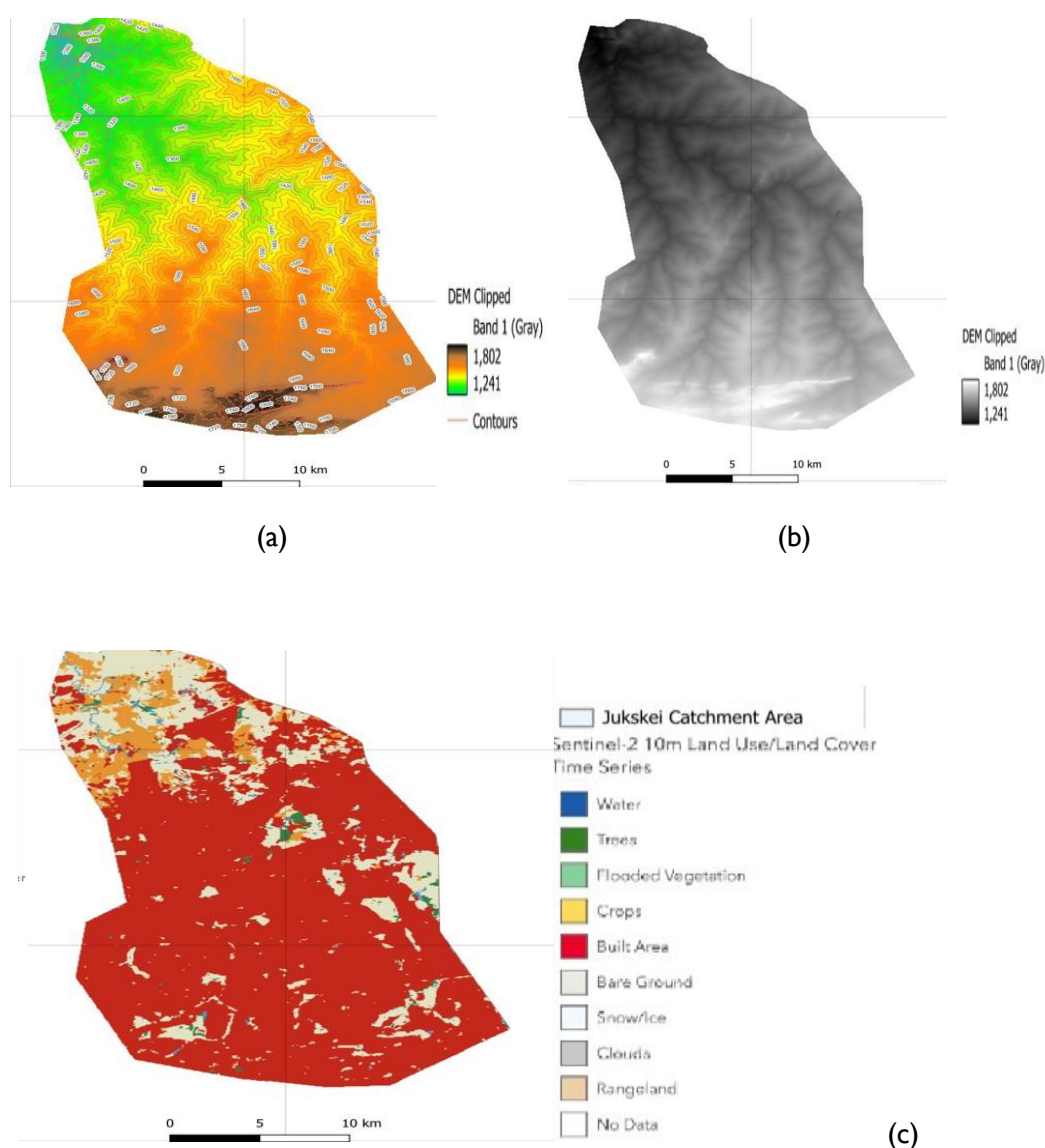


Figure 5: Showing a) SRTM DEM map and b) elevation map and c) land use map.

Using the provided rainfall data with the rational method, the flood peak discharge (Q) for The Jukskei River catchment was estimated for three return periods: 20, 50, and 100 years. The calculations are based on the rainfall intensity for these return periods, the catchment area, and a runoff coefficient for urban catchments. The statistic provided in Table 2 was used, while Gumbel distribution formula was utilized in estimating the rainfall return periods. The result from the analysis revealed a higher peak flow increases when compared with

the return period. This invariably reflects higher rainfall intensities associated with fewer and more extreme events. The flood peak discharge is a critical parameter for flood risk assessment, as it dictates the severity of flood events and the capacity required in flood management systems. In the case of the Jukskei River, the calculated flood peaks for the 20, 50, and 100-year return periods such as (1,152 m³/s, 1,280 m³/s, and 1,498 m³/s, respectively) highlight the significant risk posed by heavy rainfall in the region. This result aligned with the analysis derived from previous studies on flow peak discharge and assertions on flow peak discharge (Mawasha and Britz, 2022; Malatji, 2019). The increasing flood peak values for infrequent return periods emphasized the growing risk of flash flooding during extreme rainfall events, especially in urbanized areas like Johannesburg, where impervious surfaces contribute to rapid runoff. Similarly, base flow was equally estimated from streamflow data recorded over a period of time. Table 3 presents the annual streamflow data for the river from 2014 to 2024, which was used to estimate the base flow. Using the rank-based approach (where the flow data is ranked in descending order), the lowest flows (i.e., the minimum annual flow) are identified as indicative of base flow. In this case, the lowest flow (rank 10) observed was 7.573 m³/year, and the second lowest flow (rank 9) was 40.162 m³/year while the average Base Flow = (7.573+40.162)/2= 23.8675 m³/year.

Table 2: Return periods verse flood peak

Return Period (years)	Daily Intensity (mm)	Hourly Intensity (mm/h)	Peak Flow (Q, m ³ /s)
20	103.67	25.92	1152
50	115.22	28.81	1280
100	125.78	31.45	1498

Table 3: Streamflow data of Juskie river. Source: (SAWS), 2024

Year	Flow (m ³ /year)	Rank (M)	Inflow in descending order	Frequency (f) (N/M)	Probability (1/f x 100)
2014	313.599	1	525.65	10	10.00
2015	40.162	2	337.911	5	20.00
2016	171.151	3	313.599	3.333333	30.00
2017	311.478	4	311.478	2.5	40.00
2018	125.35	5	271.498	2	50.00
2019	271.498	6	264.773	1.666667	60.00
2021	7.573	7	171.151	1.428571	70.00
2022	525.65	8	125.35	1.25	80.00
2023	337.911	9	40.162	1.111111	90.00
2024	264.773	10	7.573	1	100.00

The hydrodynamic modeling in HEC-RAS utilized steady-state flow data to simulate flood events associated with 20, 50, and 100-year return periods. These return periods were based on rainfall intensities derived from statistical analyses using the Gumbel distribution, with peak flows of 1,152 m³/s, 1,280 m³/s, and 1,498 m³/s, respectively. The boundary conditions were defined using the normal depth method, which estimated the downstream slope as S=0.01376 based on the average gradient derived from the Profile analysis. This computation equally aligned with previous studies in literature for instance, (Maherry *et al.*, 2017; Malatji, 2019; Mawasha and Britz, 2021) who observed nearly same result using same procedure. Figure 6 shows the Geometry of Jukskei River.

The hazard maps classified inundated areas into three categories: low hazard (depths < 0.5 m), medium hazard (depths between 0.5 and 2.0 m), and high hazard (depths > 2.0 m or areas with high flow velocities). Urban areas along the Jukskei River were identified as particularly vulnerable due to high impervious surface coverage, which accelerates runoff and exceeds the capacity of drainage systems during extreme rainfall events. Similarly, the simulation in HEC-RAS modeled the Jukskei River's response to intense rainfall events with calculated intensities of 40.27 mm/h (for 241.6 mm rainfall over 6 hours) and 30.5 mm/h (for 122 mm rainfall over 4 hours). Using the river's geometric data derived from high-resolution Digital Elevation Models (DEMs), the model incorporated these rainfall intensities to estimate peak flows and simulate water surface profiles along the river. For the 241.6 mm rainfall event, the model showed significant increases in flow velocities and water surface elevations, causing extensive inundation in low-lying floodplain areas. The 122 mm event, while less severe, still resulted in considerable runoff, demonstrating the river's limited capacity to handle sudden, high-intensity flows. The outputs from the simulation identified areas most vulnerable to overflow and highlighted potential stress points in the river's drainage system, emphasizing the urgent need for infrastructure upgrades. Figure 7 (a-c) revealed flood mapping of 20 years, 50, and 100 years return period.

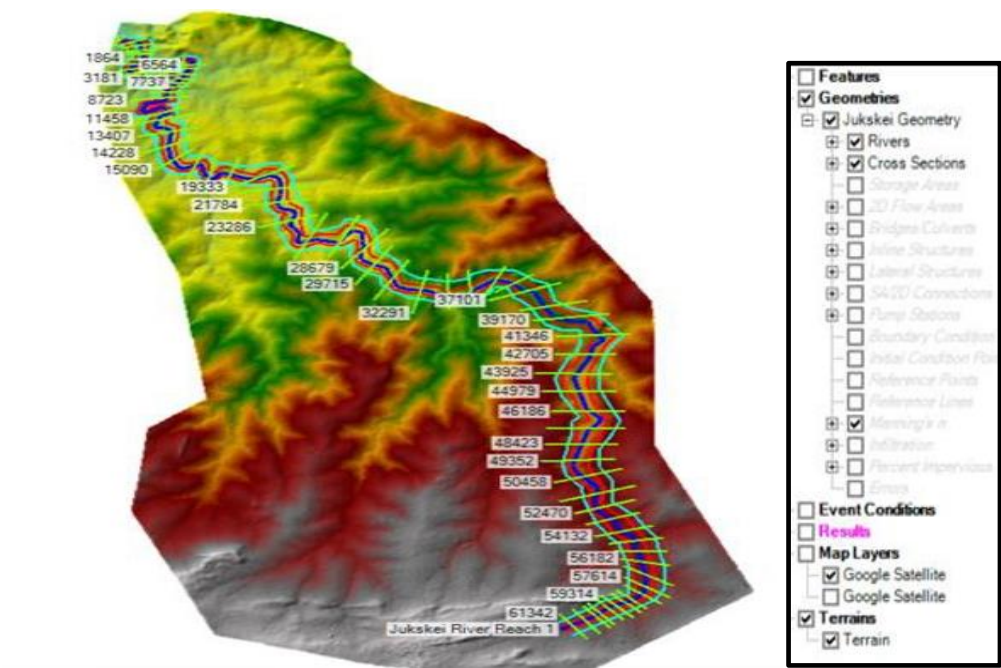
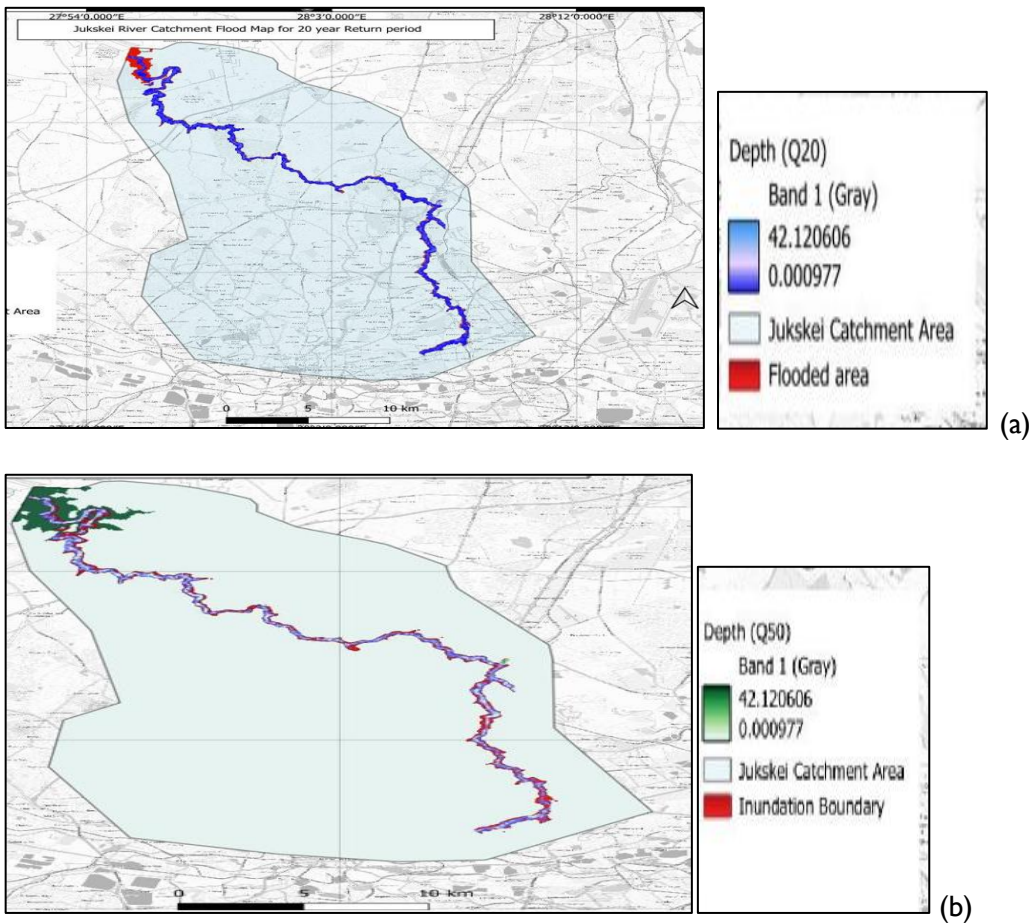


Figure 6: Geometry of Jukskei River



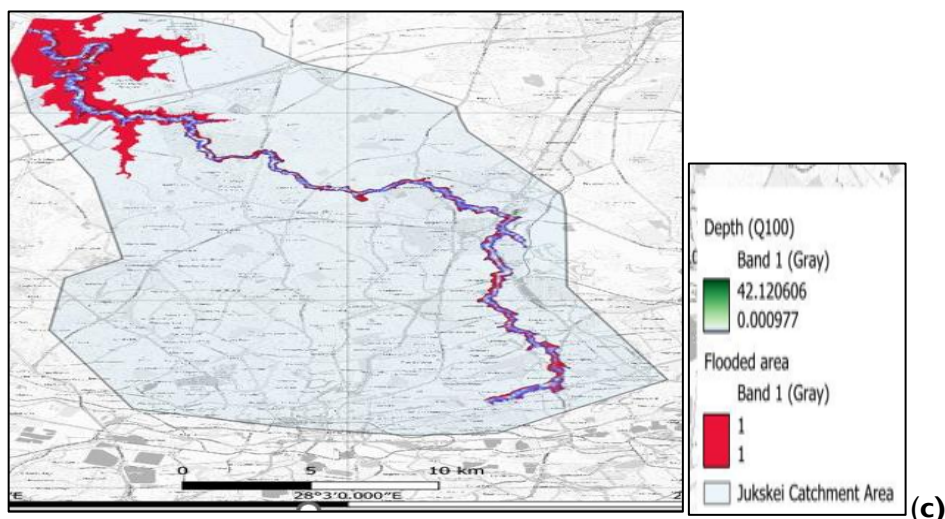


Figure 7: Flood map showing a) 20years, b) 50years c) 100-years return period

QGIS software was used to identify areas prone to overland flow accumulation, and flood extents were mapped based on the water surface elevations calculated for the 40.27 mm/h and 30.5 mm/h intensities. The mapping revealed the extent of inundation under both scenarios, with urban areas and floodplains along the river showing the highest vulnerability. The 241.6 mm rainfall event was particularly destructive, with floodwaters spilling into adjacent settlements and infrastructure. The map highlighted critical zones where water levels exceeded the riverbanks, potentially endangering residential areas and roads. For the 122 mm event, the flooding was less extensive but still posed significant risks in urbanized zones with limited drainage. These flood maps provided actionable insights into the areas at greatest risk, helping to support urban planners and emergency response teams in prioritizing mitigation and adaptation strategies. However, using two flood events for 7th 2020 and 4th December 2022 such as

Adjusted Rainfall Intensities

For 04 December 2022 Rain intensity 122 mm in 4 hours: $I = 122/4 = 30.5 \text{ mm/h}$

For 7 February 2020, $I = 241.6/6 = 40.27 \text{ mm/h}$

Calculations for Peak Flow = For $I = 30.5 \text{ mm/h}$

$Q = 0.8 \cdot 30.5 \cdot 200,000 = 4,880,000 \text{ m}^3/\text{h} = 1,356 \text{ m}^3/\text{s}$ = For $I = 40.27 \text{ mm/h}$

$= 0.8 \cdot 40.27 \cdot 200,000 = 6,443,200 \text{ m}^3/\text{h} = 1,790 \text{ m}^3/\text{s}$

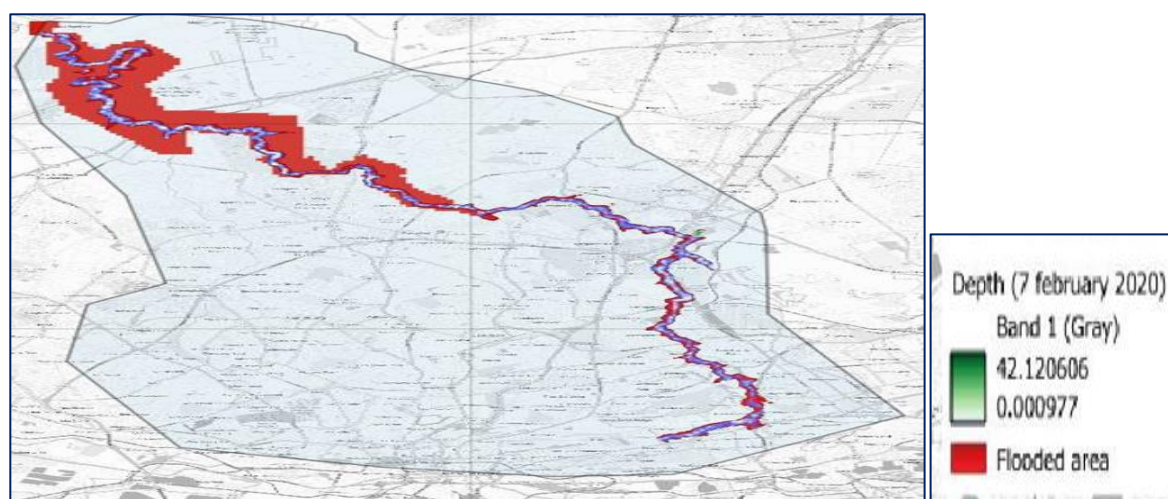


Figure 8: Flood event 7 February 2020

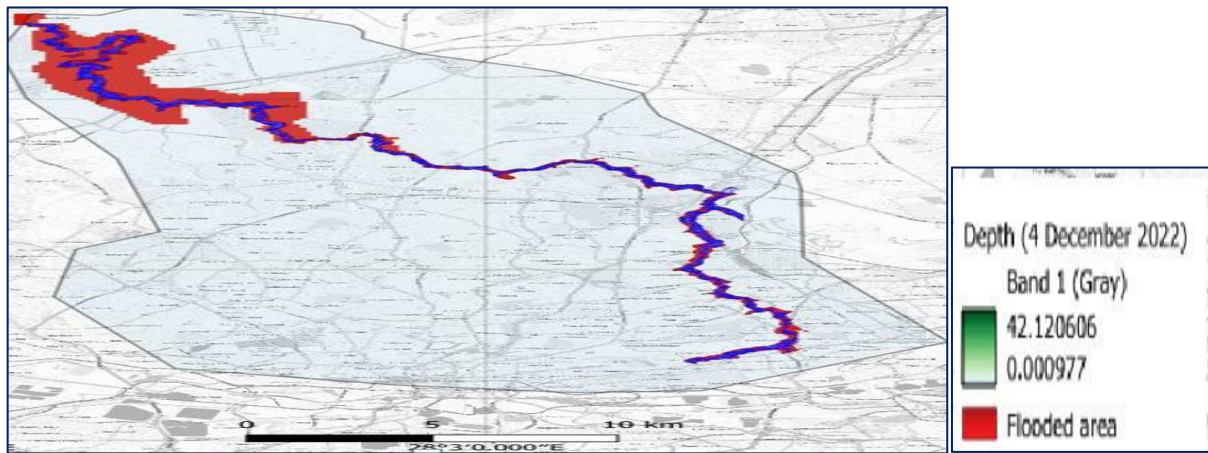


Figure 9: Flood Event 04 December 2022.

4.1 Flash Flood Validation

The rainfall events of 241.6 mm over 6 hours and 122 mm over 4 hours correspond to return periods based on the statistical rainfall intensities. The 241.6 mm event aligns closely with the intensity for a 100-year return period (125.78 mm/day or approximately 31.45 mm/h), indicating its classification as an extreme and rare flooding event. This event would result in significant overflow along the Jukskei River. Other flash flood scenario event was equally used for validation such as On February 6, 7 and 10, 2020 where South African Weather Service (SAWS) issued flood alerts as the rainfall exceeded threshold levels, signaling the potential for dangerous flooding (Scrolla.Africa, 2020, SAWS, Floodlist, Media, 2020). The records include 53.2 mm, 241.6 mm and 120.5 mm respectively. However, December 12, 2022, with record of 226.4 mm, the intense rainfall caused the Jukskei River to overflow as reported by (Ngcuka, Daily Maverick, 2022). Other recorded expanded rainfall in the same month includes December 3, 2022: 95.3 mm, December 4, 2022: 122.0 mm, December 5, 2022: 128.8 mm and December 6, 2022: 67.4 mm Figure 1 (a-e). A tragic flash flood occurred between December 3–6, 2022, when intense rainfall triggered a rapid rise in water levels along the Jukskei River, leading to fatalities. On December 6, 14 people lost their lives during a church baptism ceremony at Bramley Park. The suddenness of the flood, compounded by the rising river levels (Mawasha & Britz, 2021; Daily Maverick, 2024). The rainfall data in Figure 2 (a-e) validates the claims made by news outlets. Plate 1 and 2 depicts the physical justification of flash flood situation at Jukskei River catchment.



Plate 1: Report on rising water levels along the Jukskei river Setswetla Informal settlement, Alexandra (February, 8, 2020) (Source: Scrolla Africa, 2020, flood report)



Plate 2: Jukskei catchment situation (Source: Ngcuka, Daily Maverick 2022, flood report).

5. Conclusion

This research utilized satellite imagery and Geographic Information Systems (GIS) to analyze and map flash flood risks along the Jukskei River. Through a combination of hydrological modeling, spatial analysis, and risk mapping, the study successfully identified high-risk areas and provided insights into the factors contributing to flash flood dynamics. Rainfall events exceeding the 90th percentile threshold (112.2 mm) was found to significantly increase the likelihood of flash floods. The urban areas in the Jukskei River catchment, characterized by extensive impervious surfaces, exhibited high runoff coefficients, which compounded flood risks. Peak discharge rates calculated for 20-, 50-, and 100-year return periods showed increasing flood severity, with values of 1,152 m³/s, 1,280 m³/s, and 1,498 m³/s, respectively. These rates underline the critical need for effective urban drainage solutions to mitigate peak flows. This study faced several data constraints, including the moderate resolution of SRTM DEMs, which may not capture detailed urban features, and the temporal limitations of satellite imagery. Therefore, further research should prioritize the integration of higher-resolution datasets, such as advanced satellite imagery and LiDAR-based DEMs, to improve the accuracy of flood risk mapping and modeling.

References

- Abdelkareem, M., Al-Arifi, N., Abdalla, F., Mansour, A. and El-Baz, F. 2022. 'Fusion of remote sensing data using GIS-Based AHP-Weighted overlay techniques for groundwater sustainability in arid regions, Sustainability, 14: 7871.
- Abiye, TA. 2023. Contribution of hydrogeology to solving community water supply problems in South Africa. South African Journal of Science. 119(1/2):14599
- Agonafir, C., Lakhankar, T., Khanbilvardi, R., Krakauer, N., Radell, D. and Devineni, N. 2023. A review of recent advances in urban flood research. Water Security 19: 100141.
- Alarifi, SS., Abdelkareem, M., Abdalla, F. and Alotaibi, M. 2022. Flash flood hazard mapping using remote sensing and GIS techniques in Southwestern Saudi Arabia. Sustainability, 14:1414.
- Anaba, N., Banadda, N., Kiggundu, J., Wanyama, B., Engel and D. Moriasi. 2017. Application of SWAT to assess the effects of land use change in the Murchison Bay catchment in Uganda. Computational Water, Energy, and Environmental Engineering, 6, 24-40
- Arabameri, A., Saha, S., Chen, W., Roy, J., Pradhan, B. and Bui, D.T. 2020. Flash flood susceptibility modelling using functional tree and hybrid ensemble techniques. Journal of Hydrology, 587, 125007
- Baloyi, J., Zwane, F. and Sibanda, S. 2018. GIS-based multi-criteria analysis for flood risk assessment: A case study of the Umgeni River catchment, KwaZulu-Natal. Journal of Hydrology and Environment, 5(2): 213–226.
- Bucherei, A., Werner, M., Homberg, MV. and Tembo, S. 2022. Flash flood warnings in context: combining local knowledge and large-scale hydro-meteorological patterns, Nat. Hazards Earth Syst. Sci., 22: 461–480.

Dube, T., Mutanga, O. and Sibanda, M. 2020. Integrating radar and optical remote sensing for flood risk assessment in informal settlements: Case of the Cape Flats, Western Cape. *South African Journal of Geomatics*, 9(1): 45–60.

Franssen, HH. 2025. Historical memory in remotely sensed soil moisture can enhance flash flood modeling for headwater catchments in Germany. *Journal of Hydrology* 648: 132395.

Fadupin, OA., Ochieng, GM. and Ndege, M. 2022. Flash flood risk management in a South African Township. A case study of Alexandra. MEng Thesis: Vaal University of Technology, 216163994.

Hussein, S., Abdelkareem, M., Hussein, R and Askalany, M. 2019. Using remote sensing data for predicting potential areas to flash flood hazards and water resources. *Remote Sensing Applications: Society and Environment*. 16: 100254.

Hossein, HA. 2024. deep learning model for predicting river flood depth and extent, *Environmental modelling & software*, 145 (105): 186.

Kaplan, G. and Avdan, U. 2018. Flood Mapping Using Sentinel-1 SAR Data: A Case Study from Turkey. *Remote Sensing*, 10(11): 1744.

Lin, BQ., Zhang, DJ. and Chen, XW et al., 2021. Threshold of watershed partition in SWAT based on separating hillslope and channel sediment simulations. *Ecological Indicators*, 121:107111.

Mawasha, TS. and Britz, W. 2021. Hydrological Impacts of Land Use - Land Cover Change on Urban Flood Hazard: A Case Study of the Jukskei River in Alexandra Township, Johannesburg, South Africa. *South African Journal of Geomatics*, 10(2), 139-162

Mawasha, T. and Britz, W. 2022. Detecting land use and land cover change for a 28-year period using multi-temporal Landsat satellite images in the Jukskei River catchment, Gauteng, South Africa. *South African Journal of Geomatics*, CONSAS Conference, 11 (1): 13-29.

Malatji, R. 2019. Towards a GIS Platform for monitoring the water quality of the Jukskei River catchment: defining a sampling network [Master's Thesis, University of Witwatersrand] Wits Institutional Repository environment on DS pace, Johannesburg.

Maherry, A., Van Huyssteen, C. and Clarke, S. 2017. Flood hazard mapping in the Limpopo River basin using Sentinel-2 imagery and GIS. *International Journal of Disaster Risk Reduction*, 21: 93–102.

Moeketsi, P., Nkhonjera, GK. and Alowo R. 2022. Changes in land use land cover within the Jukskei River basin and its implications on the water availability. *IOP Conf. Series: Earth and Environmental Science*, 1087012035.

Mukherjee, F. and Singh, D. 2020. Detecting flood prone areas in Harris County: A GIS based analysis. *Geo Journal*, 85: 647–663.

Mutuvhi, T., Mhangara, P. and Ntsangase, L. 2020. Urban flood risk assessment using Sentinel-2 and GIS: A case study of the Jukskei River basin, Johannesburg. *Urban Water Journal*, 17(3): 219–234.

Ngcuka, O. (Daily Maverick, 2022), 'It's ugly, it's completely sickening,' says water expert on Joburg's rivers. Rueben, an Alex Water Warrior, next to the Jukskei River and a house teetering on the bank. (Photo: Felix Dlangamandla / Daily Maverick).

Nenweli, R., Watson, A., Brookfield, A., Münch, Z. and Chow, R. 2024. Is groundwater running out in the Western Cape, South Africa? Evaluating GRACE data to assess groundwater storage during droughts. *Journal of Hydrology: Regional Studies*, 52: 101699

Pedzisai, E. 2010. Modelling the Impact of Land Cover Change on Stormwater Runoff Using GIS and Remote Sensing: A Case Study of Upper Manyame Catchment, Zimbabwe. MSc Dissertation. University of Zimbabwe.

Razavi-Termeh, SV., Seo, M., Njaraki, AS. and Choi, S. 2023. Flash flood detection and susceptibility mapping in the Monsoon period by integration of optical and radar satellite imagery using an improvement of a sequential ensemble algorithm. *Weather and Climate Extremes*, 41: 100595.

Sellami, EM. and Rhinane, H. 2024. A modern method for building damage evaluation using deep learning approach - Case study: Flash flooding in Derna, Libya. E3S Web of Conferences 502: 03010

Sheree, B. 2024. Alexandra Water Warriors are reviving Joburg's Jukskei River, Green Guardian, South Africa.

Schlaffer, S., Matgen, P., Hollaus, M., Wagner, W. 2015. Flood detection from multi- temporal SAR data using change detection techniques. International Journal of Applied Earth Observation and Geoinformation, 38: 15-24.

Scrolla Africa, 2020. South Africa – Floods Cause Havoc in Johannesburg and Gauteng. 8th February, 2020. Retrieved on 24th August, 2024. For Afrika <https://www.forafrika.org> › south-africa › heavy-rainfal.

South Africa - Flood (SAWS, Floodlist, Media) (ECHO Daily Flash of 10 February 2020) ReliefWeb <https://reliefweb.int> › report › south-africa-flood-saws-f.

Teffo, T., Ndwandwe, CA. and Abrahams, A. 2023. Comparative functional metagenome analysis of the Jukskei River system impacted by the urbanization phenomenon. Report to the Water Research Commission.

Zebe, E. and Sivapalan, M. 2009. Threshold behavior in hydrological systems as (human) geo-ecosystems: manifestations, controls, implications. Hydrol. Earth Syst. Sci., 13: 1273–1297,